Coherent control of atomic transport in spinor optical lattices

Brian Mischuck* and Ivan H. Deutsch
University of New Mexico

Poul S. Jessen
University of Arizona

(Received 14 May 2009; revised manuscript received 30 October 2009; published 4 February 2010)

Coherent transport of atoms trapped in an optical lattice can be controlled by microwave-induced spin flips that correlate with site-to-site hopping. We study the controllability of homogeneous one-dimensional systems of noninteracting atoms in the absence of site addressability. Given these restrictions, we construct a deterministic protocol to map an initially localized Wannier state to a wave packet that is coherently distributed over n sites. As an example, we consider a one dimensional quantum walk in the presence of both realistic photon scattering and inhomogeneous broadening of the microwave transition due to the optical lattice. Using composite pulses to suppress errors, fidelities of over 95% can be achieved for a 25-step walk. We extend the protocol for state preparation to analytic solutions for arbitrary unitary maps given homogeneous systems and in the presence of time-dependent uniform forces. Such control is important for applications in quantum information processing, such as quantum computing and quantum simulations of condensed matter phenomena.

DOI: 10.1103/PhysRevA.81.023403 PACS number(s): 37.10.Jk, 03.67.Ac

I. INTRODUCTION

Neutral atoms trapped in optical lattices have emerged as a rich platform for exploring a wide variety of phenomena and devices based on coherent quantum dynamics. Examples include quantum computers [1–4], quantum simulators of condensed matter [5,6], topological quantum field theory [7,8], and quantum chaotic dynamics [9–11]. An essential ingredient in these systems is the coherent control of atomic transport in the lattice. Such transport is driven by time-dependent variations in the lattice potential and the application of external fields. In its most basic form, the atoms' ballistic tunneling between sites in a sinusoidal potential can be controlled through time-dependent modulations of the lattice depth and phase. The latter can be used to impart a time-dependent acceleration to the lattice, thereby simulating the effects of an applied electric field for electrons in a crystal that give rise to the fundamental paradigms of coherent transport in solid-state physics. Bloch oscillations [12], Wannier-Stark ladders [13], Landau-Zener tunneling [14], and dynamical localization [15] have all been demonstrated in optical lattices and explored as mechanisms for coherent control.

More complex lattice geometries introduce additional features. For example, in a lattice of double wells, one can drive transport between sites in a pairwise manner, assuming a sufficient barrier to ignore tunneling between different double wells [16–19]. In this case, the control problem is substantially simplified, as the relevant Hilbert space in a given time interval is restricted to a small discrete set of energy levels, as opposed to the infinite chain of levels in a sinusoidal lattice. Control across the entire lattice can be implemented by modifying the geometry so that the wells are alternatively coupled to all nearest neighbors [left or right in one dimension (1D)]. Double-well lattices have been explored as a platform for quantum information processing tasks such as quantum computing [20] and simulations of condensed-matter phenomena [21].

Still richer control is possible for spinor lattices where the optical potential depends on the atom's internal spin state [22]. The lattice's morphology can now be modified through variation of the laser polarization, as well as intensity, lattice phase, etc. The earliest proposals for quantum logic in optical lattices via controlled collisions involved transport of the atoms via time-dependent rotation of the direction of a laser beam's polarization [1,2,23]. Discrete time quantum walks have also been studied with atoms in spinor lattices [24] and observed in the laboratory [25]. An alternative and perhaps more robust route to coherent control of atomic transport is to use external fields to drive spin-changing transitions that are correlated with atomic motion, similar to the scheme proposed by Foot *et al.* [26]. Such protocols can make use of the tools for robust control of spins [27–29], as developed in NMR, to the control of atomic motion in the lattice.

In this article we explore methods for coherent control of atomic transport with microwave-induced spin rotations between hyperfine levels and polarization-gradient lattices. Our main focus is on controllability—how the Hamiltonian that governs the dynamics restricts the possible unitary maps that one can implement, and how to design specific wave forms to carry out a given task. We will consider here the simplest problem of noninteracting atoms in one dimension. While extensions to the interacting case are nontrivial, the current work is an important stepping stone in that direction.

The remainder of the article is organized as follows. In Sec. II we establish the formalism necessary to describe spinor lattices and their interactions with external fields. We apply this to study the conditions for wave-function control (the preparation of a desired spinor wave function starting from a known localized Wannier state) and prescribe a constructive algorithm for carrying out this task in Sec. III. We then generalize this in Sec. IV to the case of more general unitary maps for unknown initial states. Finally, we summarize and give an outlook toward future research in this area in Sec. V.

*bmischuc@unm.edu

II. MICROWAVE-DRIVEN SPINOR LATTICES

Spinor lattices arise from the tensor nature of atom-photon interaction. In a monochromatic laser field $\mathrm{Re}[(\mathbf{E}(\mathbf{x})e^{-i\omega_L t}]$, the light-shift potential takes the form

$$V_{\mathrm{LS}}(\mathbf{x}) = -\tfrac{1}{4}\alpha_{ij}E_i^*(\mathbf{x})E_j(\mathbf{x}), \tag{1}$$

where α_{ij} is the atomic dynamic polarizability at frequency ω_L for atoms in a particular ground-state manifold. In a 1D optical lattice with polarization gradients, the electric field can be written as $\mathbf{E}(z) = \boldsymbol{\epsilon}(z)E_0e^{-i\omega_L t}$, where $\boldsymbol{\epsilon}(z)$ is the local polarization vector (not normalized) and E_0 is a chosen characteristic electric field. Restricting our attention to alkali atoms, when the laser field detuning is large compared to the excited-state hyperfine splitting but not large compared to either ground-state hyperfine splitting or the fine-structure splitting, we must account for both the irreducible rank-0 (scalar) and rank-1 (vector) terms in the lift shift but can ignore the rank-2 (tensor) contribution [30]. The resulting light-shift operator for the hyperfine manifold F is

$$V_F(z) = V_F^{(0)}|\boldsymbol{\epsilon}(z)|^2 + V_F^{(1)}\left[\frac{\boldsymbol{\epsilon}^*(z)\times\boldsymbol{\epsilon}(z)}{i}\right]\cdot\mathbf{F} \tag{2a}$$

$$V_F^{(0)} = \frac{I_0}{I_{\mathrm{sat}}}\frac{\hbar\Gamma^2}{8}\left(\frac{1}{3}\frac{1}{\Delta_{F1}} + \frac{2}{3}\frac{1}{\Delta_{F2}}\right) \tag{2b}$$

$$V_F^{(1)} = \frac{g_F}{3}\frac{I_0}{I_{\mathrm{sat}}}\frac{\hbar\Gamma^2}{8}\left(\frac{1}{\Delta_{F1}} - \frac{1}{\Delta_{F2}}\right) \tag{2c}$$

where $\Delta_{F1,2}$ are the detunings of the ground-state hyperfine manifold F from the D_1 and D_2 resonances, g_F is the Landé g-factor (without nuclear magneton), $I_0 = cE_0^2/8\pi$ is the characteristic intensity of the field, and I_{sat} and Γ are, respectively, the saturation intensity and linewidth for either the D_1 or the D_2 transition. Note that the ratio $\Gamma^2/I_{\mathrm{sat}}$ depends only on the dipole matrix element and is thus same for both D_1 and D_2, so we can factor it out in this way. The ellipticity in the laser field leads to a fictitious magnetic field that varies in space and results in a spin-dependent light shift due to the rank-1 contribution [31].

We consider a 1D geometry consisting of counterpropagating laser beams with linear polarizations forming a relative angle θ (the "lin-θ-lin" geometry). The local polarization vector can be written $\boldsymbol{\epsilon}(z) = \mathbf{e}_1e^{ik_Lz} + \mathbf{e}_2e^{-ik_Lz}$, where $\mathbf{e}_1\cdot\mathbf{e}_2 = \cos\theta$ and $\mathbf{e}_1\times\mathbf{e}_2 = \sin\theta$, with I_0 chosen to be the intensity of one of the beams. Taking the atom's quantization axis along z, substituting in Eq. (2), the optical lattice for magnetic sublevel $|F,m\rangle$ is

$$V_{F,m} = 2V_F^{(0)} + A_{F,m}(\theta)\cos[2k_Lz - \delta_{F,m}(\theta)] \tag{3a}$$

$$A_{F,m}(\theta) = 2\sqrt{\left[V_F^{(0)}\right]^2\cos^2\theta + m^2\left[V_F^{(1)}\right]^2\sin^2\theta} \tag{3b}$$

$$\delta_{F,m}(\theta) = \tan^{-1}\left[\left(mV_F^{(1)}/V_F^{(0)}\right)\tan\theta\right]. \tag{3c}$$

The addition of a static bias magnetic field breaks the degeneracy between Zeeman sublevels within a manifold and allows us to spectrally isolate different microwave transitions between the manifolds. For concreteness, we consider ^{133}Cs and choose a two-state subspace $|F=4, m=3\rangle \equiv |\uparrow\rangle$, $|F=3, m=3\rangle \equiv |\downarrow\rangle$ to define a pseudospin-1/2 particle. Restricting to this subspace and adding a near-resonant microwave field with magnetic field $B_{\mu w}\cos(\omega_{\mu w}t+\phi)$ that couples these spin states, the Hamiltonian in the rotating frame takes the form $H = H_{\mathrm{latt}} + H_{\mu w}$, where

$$H_{\mathrm{latt}} = \frac{p^2}{2m} - V_0\cos(2k_Lz+\delta_0)|\uparrow\rangle\langle\uparrow| - V_0\cos(2k_Lz-\delta_0)|\downarrow\rangle\langle\downarrow| \tag{4a}$$

$$H_{\mu w} = -\frac{\Delta_{\mu w}}{2}\sigma_z - \frac{\Omega_{\mu w}}{2}(\cos\phi_{\mu w}\,\sigma_x + \sin\phi_{\mu w}\,\sigma_y). \tag{4b}$$

Here $V_0 = A_{4,3} \approx A_{3,3}$, $\delta_0 = \delta_{4,3} \approx -\delta_{3,3}$, $\Omega_{\mu w} = \langle\uparrow|\hat{\mu}|\downarrow\rangle B_{\mu w}/\hbar$ is the microwave resonant Rabi frequency, $\hat{\mu}$ is the atom's magnetic moment, $\Delta_{\mu w}$ is the microwave detuning from a hyperfine resonance defined by the untrapped atoms, $\phi_{\mu w}$ is the phase of the microwave oscillator, and the Pauli-σ operators are defined relative to the pseudospin. Note, in general $A_{F,m}$ will vary with θ. We ignore this for now and return to it later when we consider the performance of our protocol under realistic experimental conditions.

Neglecting the kinetic energy and diagonalizing the Hamiltonian leads to adiabatic or microwave-dressed potentials,

$$V_\pm(z) = -V_0\cos\delta_0\cos(2kz) \pm \frac{1}{2}\sqrt{[2V_0\sin\delta_0\sin(2kz) - \Delta_{\mu w}]^2 + \Omega_{\mu w}^2}. \tag{5}$$

At $\Delta_{\mu w} = 0$, in the lin $\perp$ lin ($\theta = \pi/2$) geometry, the adiabatic potentials yield a period $\lambda/4$ "subwavelength" lattice [32–35]. In the context of a Hubbard Hamiltonian describing interacting particles moving on a lattice [36], this configuration gives us greater freedom to independently control the site-to-site tunneling rate J and the onsite interaction strength U [37]. By employing both optical and microwave fields, the lattice depth dominates the control of U while the the applied microwave dominates control of J. Moreover, the tunneling matrix element is complex, set by the microwave phase, allowing for time-reversible tunneling and further control [38,39].

For $\theta \neq n\pi/2$, the adiabatic potentials take the form of a lattice of double-well potentials arising from the asymmetry for transport to the left vs the right. The parameters characterizing the double well, including barrier height, tunneling matrix element, and energy asymmetry ("tilt"), can be controlled through variations of lattice intensity and polarization, microwave power, and detuning. The richness of this system should enable us to control wave function coherence for spinors over multiple sites. Our early work on this subject demonstrated spinor double-well coherence driven by Larmor precession in a quasistatic magnetic field [22]. The current approach, based on applied microwave fields, should be much more robust and controllable.

While the dressed-lattice adiabatic potentials guide intuition about the transport, quantitative predictions are more accurately made by considering the band structure of the Hamiltonian, H_{latt}, in Eq. (4). Associated with the spin $s=\uparrow$ and $s=\downarrow$ lattices are Bloch states for band n and quasimomentum q, $|\psi_{n,q}^{(s)}\rangle$, and Wannier states for that band and lattice site l, $|\phi_{n,l}^{(s)}\rangle$, related by the usual Fourier transform over the first Brillouin zone,

$$\left|\phi_{n,l}^{(s)}\right\rangle = \int_{-1/2}^{1/2} e^{i2\pi lq}\left|\psi_{n,q}^{(s)}\right\rangle dq. \tag{6}$$

Here and throughout, lengths are measured in units of the lattice period $L = \lambda_L/2$ and wave numbers in units of the reciprocal lattice vector $K = 4\pi/\lambda_L$. For sufficiently deep lattices and atoms in the lowest lying bands, tunneling between sites is completely negligible over the time scales of interest. In that case, the lattice Hamiltonian is diagonal in both the Bloch and the Wannier bases, with no energy variation over the q or l index.

Transport dynamics are driven by the microwaves tuned to cause transitions between the ground bands associated with the spin-up and spin-down lattices. We assume that the detuning and Rabi frequency are sufficiently small that the single-band and lattice tight-binding (TB) model is a good approximation. Henceforth we drop the band index and set $n = 0$. To simplify notation, we set $|\phi^{(s)}_{n=0,l}\rangle = |l, s\rangle$ and $|\psi^{(s)}_{n=0,q}\rangle = |q, s\rangle$. In the Wannier basis, the total Hamiltonian in the TB approximation is

$$H_{\mathrm{TB}} = \sum_{l=-\infty}^{\infty} -\frac{\Delta_{\mu w}}{2}\sigma_z^l - \frac{1}{2}[e^{-i\phi_{\mu w}}(\Omega_R\sigma_+^{l,R} + \Omega_L\sigma_+^{l,L}) + \mathrm{H.c.}] + \mathrm{H.c.}], \tag{7}$$

where

$$\sigma_z^l \equiv |l,\uparrow\rangle\langle l,\uparrow| - |l,\downarrow\rangle\langle l,\downarrow|, \tag{8a}$$

$$\sigma_+^{l,R} \equiv |l,\uparrow\rangle\langle l,\downarrow|, \tag{8b}$$

$$\sigma_+^{l,L} \equiv |l-1,\uparrow\rangle\langle l,\downarrow| \tag{8c}$$

are the Pauli operators for two-level transitions that pairwise couple spin-down Wannier states to their neighbors on the right, $|l,\downarrow\rangle \to |l,\uparrow\rangle$, and on the left, $|l,\downarrow\rangle \to |l-1,\uparrow\rangle$. Note that we have chosen an arbitrary labeling of the Wannier state indices by convention so that a spin-down state and spin-up state to its right are both associated with the same lattice period label, l. Because the microwaves transfer negligible momentum to the atoms, translation of the atomic wave packet is possible only when the probability amplitude of an atom overlaps between neighboring sites. The Rabi frequencies for transitions to the left or right are thus weighted by Franck-Condon factors, $\Omega_R = \langle\phi_l^{\uparrow}|\phi_l^{\downarrow}\rangle\Omega_{\mu w}$, $\Omega_L = \langle\phi_{l-1}^{\uparrow}|\phi_l^{\downarrow}\rangle\Omega_{\mu w}$. For the ground bands in the TB approximation, a large asymmetry in right-left transport and isolation of double wells arises from small asymmetry in right-left displacement of the lattice due to the Gaussian overlap of the wave packets (see Fig. 1).

The combination of spinor optical lattices and microwave-driven spin dynamics provides a wide variety of parameters that can be modulated in real time during an experiment to coherently control atomic transport. In the next section we study the formal controllability of this system and develop constructive protocols to implement desired unitary maps.

III. WAVE PACKET CONTROL

Given the time-dependent Hamiltonian at hand, a first question to address is "controllability"; that is, which class of unitary transformations can be generated by the arbitrary design of the wave forms that parametrize that Hamiltonian. We consider first the problem of preparing an arbitrary wave packet that is coherently distributed over multiple sites of the lattice, starting from an initially localized Wannier state. Unless specially designed to allow for individual site addressability [4,40], control in a typical lattice is limited by translational invariance of the operations. Although a linear gradient breaks the translational symmetry, the controllability of the system is still limited, as we show later in this article. We thus restrict our attention to strictly periodic lattices and allow for an additional constant force F on the atoms, as in the case of lattices held vertically in gravity, or when the overall lattice is accelerated through time-dependent changes of the standing wave pattern.

We consider Hamiltonians that are composed of a translationally invariant part, H_0, with period L, and an applied force, F,

$$H(t) = H_0(t) + F(t)x. \tag{9}$$

A particular example is $H_0(t) = H_{\mathrm{TB}}(t)$, as given in Eq. (7), with time-dependent variations in microwave power and/or phase. The time evolution of such a system may be written in the form of the time-ordered exponential

$$U(t) = T\exp\left\{-i\int_0^t [H_0(t') + F(t')x]\,dt'\right\}. \tag{10}$$

Such a map has the property that if we translate the entire system by j times the period of H_0, then $U \to e^{-i\int_0^t F(t')dt' jL}U$. If the initial state $|\phi\rangle$ is a localized Wannier state, it satisfies

$$\langle\phi|T_j|\phi\rangle = \delta_{j,0}, \tag{11}$$

where T_j translates the system by jL. If state $|\phi\rangle$ maps to $|\phi'\rangle$ under a unitary evolution of this form, then the evolved state satisfies this same condition, as follows from the identity

$$\langle\phi'|T_j|\phi'\rangle = \langle\phi|U^\dagger T_j U|\phi\rangle = e^{i\int_0^t F(t')dt' jL}\langle\phi|T_j|\phi\rangle = \delta_{j,0}. \tag{12}$$

Thus, any wave packet prepared by these controls must be orthogonal to itself after a translation by an arbitrary number

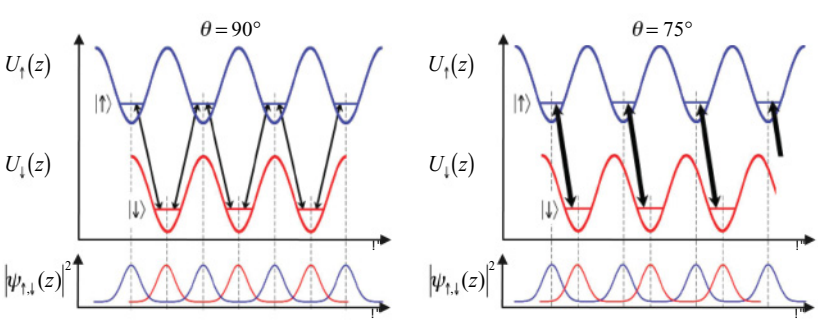

FIG. 1. (Color online) Controlled transport in lin-θ-lin. Spin-dependent lattices have a relative phase shift due to polarization gradient. In the lin ⊥ lin configuration, $\theta = 90°$, there is no asymmetry in right-left transport, and atoms can ballistically tunnel in the dressed potential. For a change of just 15° degrees away from lin ⊥ lin, in a lattice with an oscillation frequency of 35 kHz, the ratio of the effective tunelling rates is $\Omega_L/\Omega_R \approx 780$. The result is lattice of double wells with pairwise tunneling couplings.

of periods. Furthermore, since the force F has dropped out, the linear gradient does not impact the range of states that may be reached.

Are all states that satisfy this constraint reachable through some choice of the control wave forms that parametrize $H_{\rm TB}$ in Eq. (7)? To show that this is the case, we employ a protocol for constructing a desired state-to-state mapping as defined by Eberly and Law in the context of Jaynes-Cummings ladder [41]. First note that if we can map the state $|\phi\rangle$ to another state $|\phi'\rangle$ and the control Hamiltonian allows the unitary map to be time-reversible, then we can map $|\phi'\rangle$ to $|\phi\rangle$. Thus, in order to show that we can get from a localized state to any state satisfying Eq. (12), we consider the time-reversed problem of mapping such a state to the initial Wannier state.

To construct the desired map, we employ a series of SU(2) rotations on resolvable subspaces of the total Hilbert space. Such a collection of disjointed two-level systems can be addressed in a lin-θ-lin spinor lattice in either an asymmetric configuration ($\theta \neq \pi/2$) or a lin $\perp$ lin configuration in the presence a sufficiently strong uniform force so that isolated pairs of states are spectroscopically addressable (see Fig. 2). Note that in the latter case, because of the presence of an external force, if we translate the system by an integer multiple of $\lambda/2$, the state picks up an extra phase due to the linear gradient. As we will see later in this article, our construction does not require these phases, and since the construction is capable of synthesizing all reachable states, the phases are redundant. We can ignore the phases if we choose the time over which the two level unitaries operate to be an integer multiple of $2\pi/FL$, and we will assume this to be the case for the rest of this section.

We will restrict our attention to states with support strictly on a finite set of lattice sites and zero probability amplitude outside some range. Such spinors can be represented as

$$|\psi\rangle = \sum_{l=l_{\rm min}}^{l_{\rm max}} (c_{l\downarrow}|l\downarrow\rangle + c_{l\uparrow}|l\uparrow\rangle). \tag{13}$$

The finite extent of the wave function, together with the condition expressed in Eq. (12), places a constraint on the two-level subspaces. If we translate the entire state by $l_{\rm max} - l_{\rm min}$ then,

$$\langle\psi|T_{l_{\rm min}-l_{\rm max}}|\psi\rangle = c^*_{l_{\rm min}\uparrow}c_{l_{\rm max}\uparrow} + c^*_{l_{\rm min}\downarrow}c_{l_{\rm max}\downarrow} = 0. \tag{14}$$

Thus, in order to satisfy Eq. (12), the two outermost two-level subspaces must be orthogonal. Moreover, because of translational invariance, the unitary transformations that we apply are equivalent at each period of the lattice. In particular, by unitarity, if we apply a rotation operator that maps the subspace on the left end of the atomic distribution to pure spin up, the subspace at the right end of the distribution must be rotated to pure spin down.

These observations are the core of our construction (see Fig. 3). A sequence of two-level rotations can be used to map a coherent superposition delocalized across the lattice to one localized at a single site in a single spin state. In the first step, a rotation is applied to map all population at the leftmost two-level system ($l = l_{\rm min}$) to spin up according to the microwave-driven SU(2) transformation,

$$S = \frac{1}{\sqrt{N}}\begin{bmatrix} c^*_{l_{\rm min},\uparrow} & c^*_{l_{\rm min},\downarrow} \\ -c_{l_{\rm min},\downarrow} & c_{l_{\rm min},\uparrow} \end{bmatrix}, \tag{15}$$

where $N = |c_{l_{\rm min},\uparrow}|^2 + |c_{l_{\rm min},\downarrow}|^2$. By the translation symmetry this simultaneously maps all population at the rightmost two-level system ($l = l_{\rm max}$) to spin down, resulting in the spinor state

$$|\psi'\rangle = c'_{l_{\rm min}\uparrow}|l_{\rm min}\uparrow\rangle + \sum_{l=l_{\rm min}+1}^{l_{\rm max}-1}(c'_{l\downarrow}|l\downarrow\rangle + c'_{l\downarrow}|l\downarrow\rangle) + c'_{l_{\rm max}\downarrow}|l_{\rm max}\downarrow\rangle, \tag{16}$$

thereby shrinking the extent of the wave function by $\lambda/2$. The lattice is then reconfigured (through polarization rotation, a change of microwave frequency, or a change in acceleration) so that the opposite neighbors are coupled (spin down now

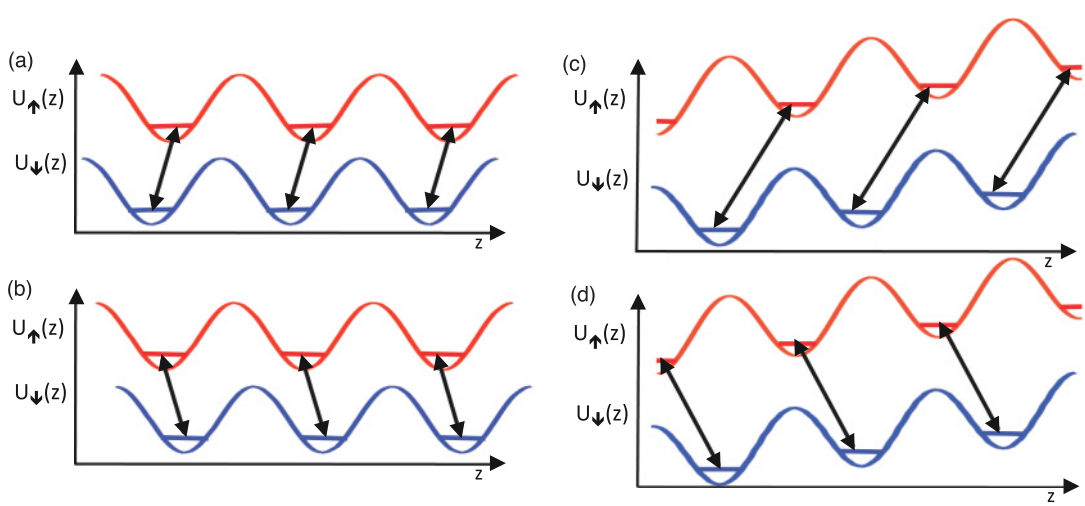

FIG. 2. (Color online) Two different methods for isolating unitary maps on two-level subspaces. In (a) and (b), the choice of polarization angles in a lin-θ-lin lattice isolate different sets of two-level systems with transport either to the right or to the left. In (c) and (d), two-level systems in a lattice with a linear gradient are spectrally addressed through their distinct microwave transition frequencies, which differ by $\pm FL/2\hbar$.

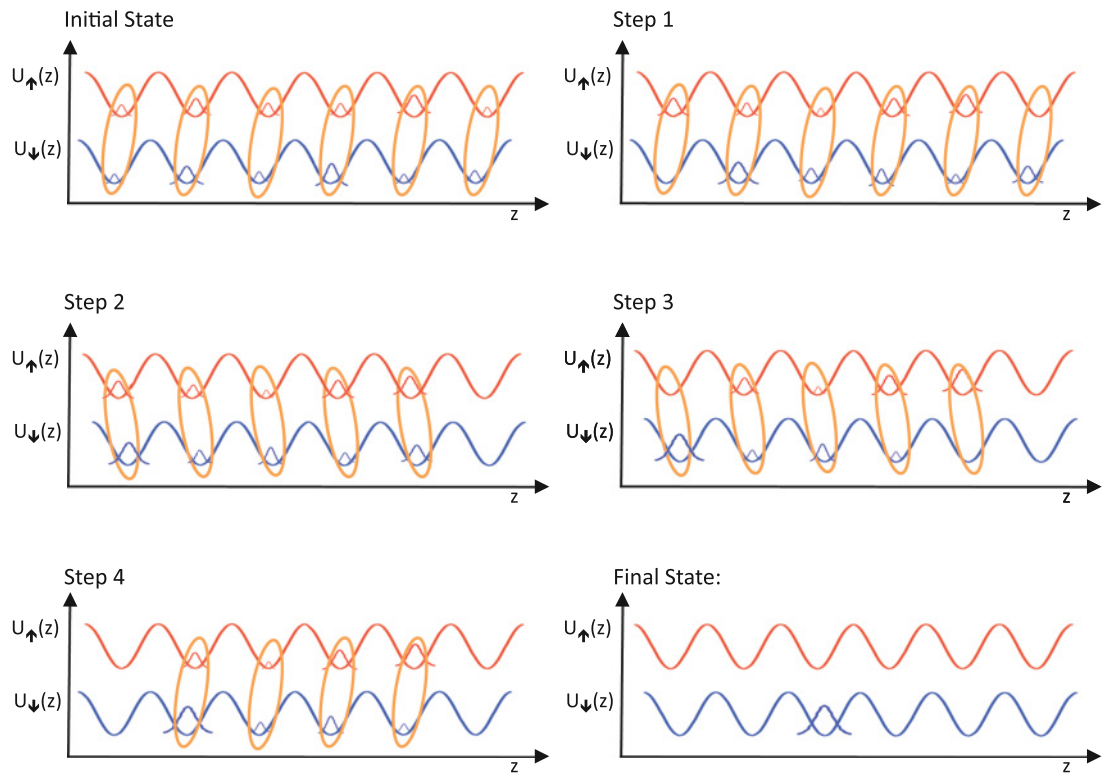

FIG. 3. (Color online) An example of state preparation through sequential SU(2) rotations. The polarization of the two counterpropagating beams is chosen to isolate sets of two-level systems. In step 1, population in the leftmost two-level system is mapped to entirely spin up, forcing population in the rightmost two level system to be entirely spin down by Eq. (14). In step 2, the polarization is rotated so that a different set of two-level systems is coupled. In step 3, the population in the leftmost level is then mapped to entirely spin down. In step 4 the polarization is set to its original configuration and steps 1–4 are repeated until the state is localized. For this particular case, we have chosen to end the sequence spin down. A different choice for the final pulse would have ended the state spin up.

coupled to spin-up neighbor on left). An appropriate SU(2) rotation is then applied to map all population on the leftmost edge to spin down (simultaneously moving all population on rightmost edge to spin up). Repeating, we form a sequence of rotations that take the outer edges of the distribution and map them inward in steps of $\lambda/4$ until all the population is localized at one Wannier state. Reversing the order of the sequence provides the desired protocol for constructing any single particle wave function in the given band and with support on a finite number of lattice sites, subject to the constraint Eq. (12).

To understand how such a protocol would perform in the laboratory, it is important to consider a variety of possible imperfections. Microwave pulse control can be achieved with extreme precision and will contribute negligibly to any infidelity in the state preparation. The residual errors thus arise from the effects of the optical lattice itself. First, to achieve sufficient localization that a single-band TB approximation is appropriate and to ensure a good double-well configuration for small rotations of the polarization away from $\theta = 90^\circ$, an intense optical lattice is required, and this will inevitably lead to photon scattering, optical pumping, and decoherence. Second, because of inhomogeneity in the laser intensity, there will generally be variations in the optical potentials as functions of position. This leads to microwave detuning variations across the lattice, as the spin-up and spin-down states see differential light shifts that vary from site to site. Moreover, the atomic localization will vary over the lattice, and thus so will the Frank-Condon overlap, leading to errors in the effective microwave Rabi frequencies $\Omega_{L,R}$. Finally, as the lattice polarization is rotated and the spin-up and spin-down optical potentials translated relative to each other, the spin-up and spin-down states will accumulate differential phase shifts that vary from site to site. This is equivalent to inhomogeneous microwave phase errors during subsequent pulses.

In principle, tools such as composite pulses and spin echoes can be employed to mitigate some of these errors. The NMR community has developed a variety of pulse families that are designed to be robust under different circumstances. We consider three examples: CORPSE, SCROFULOUS, and BB1 [27,28,42]. CORPSE is a composite pulse which is designed to be robust to detuning errors to fourth order, while SCROFULOUS and BB1 are composite pulses which are designed to be robust to errors in the Rabi frequency to fourth and sixth order, respectively. At the same time, CORPSE will perform roughly as well as uncompensated (plain) pulses with respect to errors in the Rabi frequency, while BB1 will perform roughly as well as plain pulses and SCROFULOUS will perform worse than plain pulses with respect to errors in the detuning. One drawback to all composite pulses is that they require more time to implement than plain pulses. In the presence of photon scattering, this can degrade the performance of composite pulses and ultimately make them perform worse than the shorter plain pulses [29].

To illustrate the various tradeoffs, we consider a quantum walk implemented by alternating microwave pulse sequences with rotations of the lattice polarization to the left- and right-coupling configurations (Fig. 2). The microwave pulses are chosen to generate a $\pi/2$ rotation of the pseudospin on the Bloch sphere about the x axis, using either a single plain pulse or one of the three composite sequences discussed earlier in this article. We choose the optical lattice to have a wavelength of 865 nm and a mean intensity of 250 W/cm^2, similar to the parameters used in a recent transport experiment by Widera *et al.* [25]. Atoms are transported to the left and right by toggling the polarization angle between $\theta_L = 75^\circ$ and $\theta_R = 105^\circ$. For these parameters, and working with a pseudospin composed of the states $|F = 4, m_F = 3\rangle$ and $|F = 3, m_F = 3\rangle$, the atomic oscillation frequency in the lattice potential wells is 35 kHz and the photon scattering time is $t_s = 1.3$ s. Also, the ratio of Ω_L to Ω_R, or vice versa, is equal to 780 when the lattice angle is in left- or right-coupling configuration, ensuring a lattice of highly isolated double wells. For the microwave drive we choose the free-space pseudospin Rabi frequency to be $\Omega_{\mu w} = 5.9$ kHz; this leads to an effective Rabi frequency in the lattice of $\Omega_{L,R} = 1.0$ kHz due to the Franck-Condon factor. To confirm that the single-band approximation is valid for these parameters, we studied a simple four-level model that included the two lowest Wannier states for each spin. In that case, starting from the spin-down ground Wannier state and driving microwave transitions to the spin-up ground Wannier states for a time much longer than the effective Rabi periods, the populations in the first excited Wannier states never exceed 0.95%.

To model the lattice inhomogeneity, we assume a Gaussian spread in laser intensities with a standard deviation of 2.5% about the mean. This leads to a spread in the effective microwave Rabi frequencies due to Franck-Condon inhomogeneity, $\delta\Omega_{R,L} = 24$ Hz, and a spread of microwave detunings due to the spread of differential light shifts, $\delta\Delta_{\mu w} = 8.8$ Hz. In addition, the relative phase accumulated between spin-up and spin-down states due to the variation of potential depths during transport averages $8 \times 10^{-4\,\circ}$, with a spread of $\delta\phi_{\mu w} = 0.002^\circ$ due to lattice inhomogeneity. To determine the effect of these errors, we evolve a pseudospin through a series of lattice polarization rotations and microwave pulses for a given lattice intensity and calculate the fidelity of the resulting state relative to the target state after each rotation-and-pulse step in the quantum walk. The overall fidelity is then obtained by averaging a number of such calculations over the distribution of lattice intensities. To account for the effects of light scattering, we multiply the fidelity by a factor of e^{-nT/t_s}, where T is the time required for a single step in the quantum walk and n is the number of such steps. For the different pulse types we have $T_{\text{plain}} = 4 \times 10^{-4} t_s$, $T_{\text{CORPSE}} = 2.9 \times 10^{-3} t_s$, $T_{\text{SCROFULOUS}} = 1.7 \times 10^{-3} t_s$ and $T_{\text{BB1}} = 3.3 \times 10^{-3} t_s$, where t_s is the photon scattering time.

The results are shown in Fig. 4. We find that SCROFULOUS and BB1 outperform CORPSE and plain pulses, which suggests that the dominant error is the spread in Rabi frequencies, even though $\delta\Omega_{R,L}$ is only about 2.7 times greater than $\delta\Delta_{\mu w}$. To see why this is the case, consider the effect of a spread in Rabi frequencies and a spread in detunings on the generalized Rabi frequency,

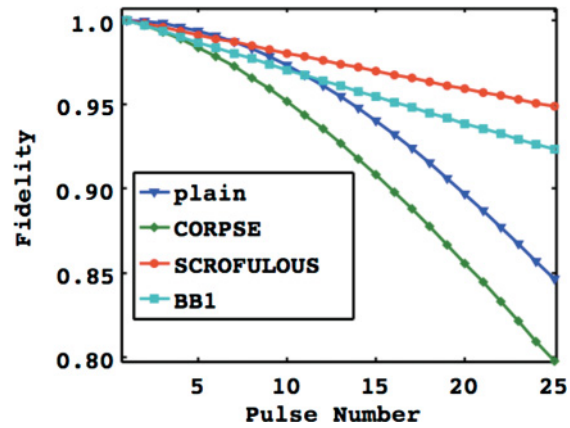

FIG. 4. (Color online) Fidelity of a quantum walk as function of number of steps for four different pulse sequences. CORPSE corrects detuning errors up to fourth order, SCROFULOUS corrects errors in the generalized Rabi frequency up to fourth order, and BB1corrects errors in the generalized Rabi frequency up to sixth order but takes longer to perform than SCROFULOUS. Because errors in the generalized Rabi frequency and decoherence by photon scattering are the dominate errors, SCROFULOUS performs the best.

$\tilde{\Omega}_{L,R} = \sqrt{(\Omega_{L,R} + \delta\Omega_{L,R})^2 + \delta\Delta_{\mu w}^2}$, where $\Omega_{L,R}$ is the mean Rabi frequency. If the generalized Rabi frequency is expanded to lowest nonvanishing order, it is first order in $\delta\Omega_{L,R}$ and second order in $\delta\Delta_{\mu w}$. As a result, the spread in effective Rabi frequencies will have greater impact than the spread in detunings. We also see that SCROFULOUS outperforms BB1 because decoherence by photon scattering is not negligible. After 25 left-right steps, the fidelity for SCROFULOUS is 95%, nearly 10% greater than the fidelity of plain pulses. In general, different lattice configurations—lattice intensity, detuning, rotation angle, etc.—will have different tradeoffs. Nevertheless, the example considered here demonstrates that high-fidelity coherent transport can be achieved within the accessible range of experimental parameters.

IV. IMPLEMENTING GENERAL UNITARY TRANSFORMATIONS

In the previous section we studied the construction of a particular unitary transformation—mapping an initially localized Wannier state to a spinor wave function delocalized over a finite number of lattice sites, under the constraint of Eq. (12). In this section we consider the most general unitary map that we can implement under these constraints. We begin with the case of perfect translational invariance of the lattice. In addition, since the microwave photons possess negligible momentum, only Bloch states with the same quasimomentum are coupled. Because of these symmetries, any unitarity transformation that we can synthesize will be block diagonal in the Bloch basis, where each block is a U(2) matrix that connects spin-up and spin-down states with the same quasimomentum q. In the basis $\{|q, \uparrow\rangle, |q, \downarrow\rangle\}$, these blocks take the form

$$U_q = e^{i\gamma(q)} \begin{bmatrix} \alpha(q) & -\beta^*(q) \\ \beta(q) & \alpha^*(q) \end{bmatrix}, \tag{17}$$

where $|\alpha(q)|^2 + |\beta(q)|^2 = 1$. If the two lattices are sufficiently deep, tunneling is suppressed so γ is independent of q and can be factored out of the problem, leading to SU(2) rotations in each block.

The decomposition of a translationally invariant unitary transformation into blocks of SU(2) matrices has important implications for the design of arbitrary maps. Generally, the design of a time-dependent wave form that generates an arbitrary unitary map is substantially more complex than a protocol for state-to-state mapping on an initially known state [43]. Intuitively, this is because state-to-state maps only constrain one column of a unitary matrix, whereas the evolution of the orthogonal complement is not fully specified. The exception is for a spin-1/2 system. By unitarity, specifying one column of an SU(2) matrix necessarily constrains the other. Since our spinor lattice is described by a collection of noninteracting spin-1/2 subspaces labeled by quasimomentum q, if we specify a state-to-state mapping of a spinor Bloch state, we specify the SU(2) matrix on this block. We can achieve this using the state-mapping protocol defined in Sec. III that takes an initially localized Wannier state to a state distributed over a finite number of lattice sites. Such a map specifies a transformation on each Bloch state according to the Fourier relationship between the probability amplitudes in the Wannier and the Bloch bases. Based on this relationship, we can use our state-to-state map to design a more general class of unitary maps on the wave function.

To see this explicitly, consider the unitary evolution of an initial spin-up Wannier state (take $l = 0$ without loss of generality):

$$\begin{aligned} U|0,\uparrow\rangle &= \int_{-1/2}^{1/2} dq[\alpha(q)|q,\uparrow\rangle + \beta(q)|q,\downarrow\rangle] \\ &= \sum_{l=-\infty}^{\infty} (c_{l,\uparrow}|l,\uparrow\rangle + c_{l,\downarrow}|l,\downarrow\rangle). \end{aligned} \tag{18}$$

The quasimomentum functions $\alpha(q)$ and $\beta(q)$ in Eq. (17) are the Fourier sums of probability amplitudes in Wannier space,

$$\alpha(q) = \sum_{l=-\infty}^{\infty} c_{l,\uparrow} e^{-i2\pi lq}, \quad \beta(q) = \sum_{l=-\infty}^{\infty} c_{l,\downarrow} e^{-i2\pi lq}. \tag{19}$$

As long as the Fourier transform of $\alpha(q)$ and $\beta(q)$ have support only over a finite extent in l, we can generate these functions by applying the state-mapping protocol of the previous section to synthesize the probability amplitudes c_l in Eq. (19). For unitary maps defined by $\alpha(q)$ and $\beta(q)$ whose Fourier expansion in Wannier states does not have a strictly finite support, more general control methods are required.

We can easily generalize our result to include control through applied spatially uniform (possibly time-dependent) forces. In the TB approximation, expressed in the Wannier basis, the Hamiltonian for a linear gradient potential in dimensionless units takes the form

$$H_{\text{grad}}(t) = \sum_{l=-\infty}^{\infty} -F(t)L[l|l\downarrow\rangle\langle l\downarrow| + [l + \delta l(t)]|l\uparrow\rangle\langle l\uparrow|], \tag{20}$$

where $\delta l(t)$ arises due to the offset between spin-up and spin-down lattices. We allow for modulations of the overall force as studied in "shaken lattices" [44–48] and the possibility of time-dependent variations in the relative positions of the two spin states, as could be implemented through modulations in the laser beams' polarization direction. The combination of this Hamiltonian, together with microwave-driven control described by H_{TB} in Eq. (7), gives rise to a general unitary transformation that can be written using the interaction picture in the form

$$U(t) = D(t)U_I(t), \tag{21}$$

where

$$D(t) = e^{-i\int_0^t H_{\text{grad}}(t')dt'} = e^{i\chi/2} \int_{-1/2}^{1/2} dq|q+\eta\rangle\langle q| \otimes e^{i\chi\sigma_z/2}, \tag{22}$$

where $\chi = \int_0^t \delta l(t')F(t')L\,dt'$, $\eta = \int_0^t F(t')dt'$, with $q + \eta$ is taken in the first Brillouin zone and

$$i\frac{d}{dt}U_I(t) = H_I(t)U_I(t), \tag{23}$$

where $H_I(t) = D^\dagger(t)H_{\text{TB}}(t)D(t)$. The exact form of H_I is rather complicated, but all that really matters for our argument is that it is translationally invariant with the period of the lattice, $T_j^\dagger H_I(t)T_j = H_I(t)$. As a result, the solution, $U_I(t)$ will be block diagonal in quasimomentum space, with the blocks consisting of SU(2) rotations. Thus, by Eq. (21), the general unitary evolution will have the form

$$U(t) = e^{i\chi/2} \int_{-1/2}^{1/2} dq|q+\eta\rangle\langle q| \otimes U_q. \tag{24}$$

A control sequence of microwave-driven rotations in a uniform lattice followed by a time-dependent linear gradient can reach any unitary map of this form.

We contrast this control with that achievable in a 1D sinusoidal optical lattice with time-dependent uniform forces and modulation of the lattice depth in the TB approximation, without symmetry breaking for right vs left transport. Haroutyunyan and Nienhuis derived a general expression for the propagator in such a situation [49]. In the quasimomentum basis, the map is

$$U(t)|q\rangle = e^{-ia(t)\cos[2\pi q - b(t)]}|q-\eta\rangle, \tag{25}$$

where

$$a(t)e^{ib(t)} = \int_0^t dt'\,\Omega(t')e^{i\eta(t')}, \tag{26}$$

$\Omega(t)$ is the hopping rate between sites (symmetric to the left or to the right), and $\eta(t)$ is the same as above. The effect of the propagator is solely to induce a phase that varies as the first-order Fourier coefficient, in addition to shifting all of the quasimomentum by an amount η. In contrast, Eq. (24) allows a broader class of unitaries to be synthesized.

V. SUMMARY AND OUTLOOK

We have described the control of transport of atoms through a microwave-dressed spinor optical lattice. Asymmetric lattices and spectral isolation provides a means to

break the system up into a series of two-level systems, which aided the design of control routines. We restricted our attention to translationally invariant systems, with no local addressing, but the possibility of a uniform applied time-dependent force. Under these conditions, we can determine the constraints of reachable states and more general reachable unitary maps that take a localized atom at one site to a state coherently extended over n sites. Based on these constraints, we propose a constructive protocol for carrying out these control tasks through a sequence of SU(2) rotations acting in the two-level subspaces. An important consideration for practical implementation of our protocol is robustness of the control sequences to imperfections in the system. Because single-particle transport is driven by a series of SU(2) maps, certain errors may be fixed by borrowing techniques from robust control of NMR systems. We have shown how errors in the lattice intensity can be corrected with such techniques. Additional errors from spatial variations or miscalibrations in the microwave field strength and real magnetic fields can also be corrected. On the other hand, the inevitable spatial inhomogeneities in the lattice potential can lead to spatial variations in the energy common to both of the levels, which causes an overall phase on the two-level systems that varies in space. Because this phase error is not an SU(2) map, it cannot be removed with the standard NMR composite pulse protocols nor their generalizations, and we must develop new methods to correct this in order to make our protocol robust to lattice inhomogeneity. This will be a topic of future investigation. In the current work we restricted our attention to the single-band, TB approximation, in uniform lattices with two spin levels. More general protocols that do not restrict the bands can be used to study the control of coupled spin and spatial degrees of freedom in a broader context. Moreover, it has recently been shown [50] that the entire hyperfine manifold of magnetic sublevels is controllable with applied rf and microwave wave forms, leaving open the possibility of combining the control of high dimensional spin and spatial degrees of freedom. In addition, breaking the translational invariance with quadratic or higher-order potentials should allow the controllability of the system to be significantly enhanced. Other modifications of the spin-dependent potentials, such as the spatial variation in microwave transition frequency that arises in a strong magnetic field gradient, can in principle allow spectral addressing of individual two-level systems and extend the controllability of the system.

Finally, the techniques proposed here may also be extended to control the dynamics of many-body systems. For instance, it might be possible to use the microwave drive to synthesize more arbitrary interactions between atoms than are dictated by the static Hamiltonian. Once interactions are included in the model, many-body unitary maps can by built from maps acting on restricted subspaces, as we have done here for single particles. Such tools can play an essential role in quantum simulations of many-body Hamiltonians, both for studies of equilibrium properties such as the many-body phase diagram and nonequilibrium phenomena such as Loschmidt echoes [38] and the dynamics of phase transitions.

ACKNOWLEDGMENTS

We thank Seth Merkel and Jae Hoon Lee for helpful discussions. This research was supported by NSF Grant Nos. PHY-0555573 and PHY-0555673 and IARPA/NIST Grant No. 70NANB4H1096.

[1] G. K. Brennen, C. M. Caves, P. S. Jessen, and I. H. Deutsch, Phys. Rev. Lett. **82**, 1060 (1999).
[2] D. Jaksch, H. Briegel, J. I. Cirac, C. W. Gardiner, and P. Zoller, Phys. Rev. Lett. **82**, 1975 (1999).
[3] O. Mandel, M. Greiner, A. Widera, T. Rom, T. W. Hansch, and I. Bloch, Nature (London) **425**, 937 (2003).
[4] K. D. Nelson, X. Li, and D. S. Weiss, Nat. Phys. **3**, 556 (2007).
[5] D. Jaksch and P. Zoller, Ann. Phys. **315**, 52 (2005).
[6] M. Lewenstein, A. Sanpera, V. Ahufinger, B. Damski, A. Sen, and U. Sen, Adv. Phys. **56**, 243 (2007).
[7] L. Duan, E. Demler, and M. D. Lukin, Phys. Rev. Lett. **91**, 090402 (2003).
[8] A. Micheli, G. K. Brennen, and P. Zoller, Nat. Phys. **2**, 341 (2006), ISSN 1745-2473.
[9] D. A. Steck, W. H. Oskay, and M. G. Raizen, Science **293**, 274 (2001).
[10] S. Ghose, P. M. Alsing, and I. H. Deutsch, Phys. Rev. E **64**, 056119 (2001).
[11] V. Y. Argonov and S. V. Prants, Europhys. Lett. **81**, 24003 (2008).
[12] M. B. Dahan, E. Peik, J. Reichel, Y. Castin, and C. Salomon, Phys. Rev. Lett. **76**, 4508 (1996).
[13] S. R. Wilkinson, C. F. Bharucha, K. W. Madison, Q. Niu, and M. G. Raizen, Phys. Rev. Lett. **76**, 4512 (1996).
[14] A. Zenesini, H. Lignier, G. Tayebirad, J. Radogostowicz, D. Ciampini, R. Mannella, S. Wimberger, O. Morsch, and E. Arimondo, Phys. Rev. Lett. **103**, 090403 (2009).
[15] K. W. Madison, M. C. Fischer, R. B. Diener, Q. Niu, and M. G. Raizen, Phys. Rev. Lett. **81**, 5093 (1998).
[16] J. Sebby-Strabley, M. Anderlini, P. S. Jessen, and J. V. Porto, Phys. Rev. A **73**, 033605 (2006).
[17] S. Folling, S. Trotzky, P. Cheinet, M. Feld, R. Saers, A. Widera, T. Muller, and I. Bloch, Nature (London) **448**, 1029 (2007), ISSN 0028-0836.
[18] O. Romero Isart and J. J. Garcia-Ripoll, Phys. Rev. A **76**, 052304 (2007).
[19] G. De Chiara, T. Calarco, M. Anderlini, S. Montangero, P. J. Lee, L. Brown, W. D. Phillips, and J. V. Porto, Phys. Rev. A **77**, 052333 (2008).
[20] M. Anderlini, P. J. Lee, B. L. Brown, J. Sebby-Strabley, W. D. Phillips, and J. V. Porto, Nature (London) **448**, 452 (2007).
[21] I. Bloch, Nature (London) **453**, 1016 (2008).
[22] D. L. Haycock, P. M. Alsing, I. H. Deutsch, J. Grondalski, and P. S. Jessen, Phys. Rev. Lett. **85**, 3365 (2000).
[23] O. Mandel, M. Greiner, A. Widera, T. Rom, T. W. Hänsch, and I. Bloch, Phys. Rev. Lett. **91**, 010407 (2003).

[24] W. Dr, R. Raussendorf, V. M. Kendon, and H. Briegel, Phys. Rev. A **66**, 052319 (2002).
[25] M. Karski, L. Forster, J. Choi, A. Steffen, W. Alt, D. Meschede, and A. Widera, Science **325**, 174 (2009).
[26] A. Deb, G. Smirne, R. Godun, and C. Foot, J. Phys. B: At. Mol. Opt. Phys. **40**, 4131 (2007).
[27] L. M. K. Vandersypen and I. L. Chuang, Rev. Mod. Phys. **76**, 1037 (2005).
[28] J. Li and N. Khaneja, Phys. Rev. A **73**, 030302(R) (2006).
[29] W. Rakreungdet, J. H. Lee, K. F. Lee, B. E. Mischuck, E. Montano, and P. S. Jessen, Phys. Rev. A **79**, 022316 (2009).
[30] I. H. Deutsch and P. S. Jessen, Opt. Commun. **283**, 681 (2010).
[31] I. H. Deutsch and P. S. Jessen, Phys. Rev. A **57**, 1972 (1998).
[32] N. Lundblad, P. J. Lee, I. B. Spielman, B. L. Brown, W. D. Phillips, and J. V. Porto, Phys. Rev. Lett. **100**, 150401 (2008).
[33] W. Yi, A. J. Daley, G. Pupillo, and P. Zoller, New J. Phys. **10**, 073015 (2008).
[34] M. Shotter, D. Trypogeorgos, and C. Foot, Phys. Rev. A **78**, 051602(R) (2008).
[35] T. Salger, G. Ritt, C. Geckeler, S. Kling, and M. Weitz, Phys. Rev. A **79**, 011605(R) (2009).
[36] D. Jaksch, C. Bruder, J. I. Cirac, C. W. Gardiner, and P. Zoller, Phys. Rev. Lett. **81**, 3108 (1998).
[37] A. Zenesini, H. Lignier, D. Ciampini, O. Morsch, and E. Arimondo, Phys. Rev. Lett. **102**, 100403 (2009).
[38] F. M. Cucchietti, e-print arXiv:quant-ph/0609202.
[39] A. Alberti, G. Ferrari, V. V. Ivanov, M. L. Chiofalo, and G. M. Tino, e-print arXiv:0903.0724.
[40] C. Zhang, S. L. Rolston, and S. D. Sarma, Phys. Rev. A **74**, 042316 (2006).
[41] C. K. Law and J. H. Eberly, Phys. Rev. Lett. **76**, 1055 (1996).
[42] H. K. Cummins, G. Llewellyn, and J. A. Jones, Phys. Rev. A **67**, 042308 (2003).
[43] K. Moore, M. Hsieh, and H. Rabitz, J. Chem. Phys. **128**, 154117 (2008).
[44] A. Zenesini, H. Lignier, D. Ciampini, O. Morsch, and E. Arimondo, Phys. Rev. Lett. **102**, 100403 (2009).
[45] V. V. Ivanov, A. Alberti, M. Schioppo, G. Ferrari, M. Artoni, M. L. Chiofalo, and G. M. Tino, Phys. Rev. Lett. **100**, 043602 (2008).
[46] A. Alberti, V. V. Ivanov, G. M. Tino, and G. Ferrari, Nat. Phys. **5**(8), 547 (2009).
[47] A. Eckardt, M. Holthaus, H. Lignier, A. Zenesini, D. Ciampini, O. Morsch, and E. Arimondo, Phys. Rev. A **79**, 013611 (2009).
[48] C. Sias, H. Lignier, Y. P. Singh, A. Zenesini, D. Ciampini, O. Morsch, and E. Arimondo, Phys. Rev. Lett. **100**, 040404 (2008).
[49] H. L. Haroutyunyan and G. Nienhuis, Phys. Rev. A **64**, 033424 (2001).
[50] S. T. Merkel, P. S. Jessen, and I. H. Deutsch, Phys. Rev. A **78**, 023404 (2008).